ORIGINAL PAPER

pH-Dependent Conformational Transitions in Conalbumin (Ovotransferrin), a Metalloproteinase from Hen Egg White

**Gulam Rabbani · Ejaz Ahmad · Nida Zaidi ·
Rizwan Hasan Khan**

Abstract Acid unfolding pathway of conalbumin (CA), a monomeric glycoprotein from hen egg white, has been investigated using far- and near-UV CD spectroscopy, intrinsic fluorescence emission, extrinsic fluorescence probe 1-anilino-8-napthalene sulfonate (ANS) and dynamic light scattering (DLS). We observe pH-dependent changes in secondary and tertiary structure of CA. It has native-like α-helical secondary structure at pH 4.0 but loss structure at pH 3.0. The CA existed exclusively as a pre-molten globule state and molten globule state in solution at pH 4.0 and pH 3.0, respectively. The effect of pH on the conformation and thermostability of CA points toward its heat resistance at neutral pH. DLS results show that MG state existed as compact form in aqueous solutions with hydrodynamic radii of 4.7 nm. Quenching of tryptophan fluorescence by acrylamide further confirmed the accumulation of an intermediate state, partly unfolded, in-between native and unfolded states.

Keywords Conalbumin · DLS · Hydrodynamic radii · Molten globule · pH denaturation · Translational diffusion coefficients

Abbreviations
ANS   1-anilino-8-napthalene sulfonate
CA   Conalbumin
DLS   Dynamic light scattering
GnHCl Guanidine hydrochloride
MG   Molten globule
MRE   Mean residue ellipticity
P_d Polydispersity
T_m Mid-point temperature

Introduction

Equilibrium and kinetic intermediates have been identified in the unfolding/refolding reactions of several proteins [1–3]. Several globular proteins when exposed to extreme pH conditions undergo significant conformational changes resulting in formation of intermediate states, with varying stability, such as molten globule (MG) state. Structural characterization of intermediates or MG state that populate in the folding/unfolding process is essential to understand the protein folding mechanism [4]. At MG state, the protein retains most of the secondary structures, but has a tendency to lose some of the tertiary structures [5–7]. The MG states are believed to be general folding intermediates because they populate both in the equilibrium and kinetic folding/unfolding pathways [8].

Egg white proteins are considered model of choice for studying proteins because of their high nutritional and biological value [9]. Conalbumin (CA), one of the main iron-binding monomeric glycoproteins containing D-mannose and D-galactose sugar moiety, is present in egg white. It transports and scavenges Fe(III) in poultry eggs. It belongs to transferrin family and exhibits features typical for α-helical proteins. The function of CA is generally accepted as that of iron transport. It binds two atoms of Fe(III), one in each domain. The order of iron binding is pH dependent; at pH 6.0, it binds first to the C-domain, but at pH 8.5, it first binds to the N-domain. It is a major contributor to the natural defense system in egg white, which provides protective barrier against infection by microbial flora [10]. An important

G. Rabbani · E. Ahmad · N. Zaidi · R. H. Khan (✉)
Interdisciplinary Biotechnology Unit, Aligarh Muslim
University, Aligarh 202 002, India
e-mail: rizwanhkhan@hotmail.com

element of this natural immunity is CA, a protein with antibacterial and antiviral properties [11]. The protein contains an N- and a C-terminal domain with six disulfide bridges in former and nine in later. These disulfide bonds form the basis of high structural stability of CA [12].

The primary goal of this work is to provide insight of folding/unfolding process induced by pH variation using a variety spectroscopic tool. The secondary and tertiary structural changes accompanying pH variation using primarily spectroscopic techniques such as far- and near-UV circular dichroism (CD), intrinsic and extrinsic fluorescence measurements while variation in hydrodynamic radii (R_h) and translational diffusion coefficient $\left(D_W^{25°C}\right)$ on different pH are analyzed by DLS measurements. The effects of pH on the protein thermal stability are further evaluated using far-UV CD at 222 nm. The conformational stability curve is calculated from two-state unfolding model [13]. The results of fluorescence emission as well as far- and near-UV CD spectroscopic studies indicated that pH-induced unfolding causes pronounced changes in the tertiary structure. We have characterized the MG state at pH 3.0 where tertiary structures were almost completely lost without major alterations at the secondary structure. Furthermore to investigate the possibility of conformational alterations in CA, we evaluated the accessibility of tryptophan residues using acrylamide as a fluorescence quencher.

Experimental Section

Iron-free conalbumin from chicken egg white (C 0755), guanidine hydrochloride (GnHCl) and 1-anilinonaphthalene-8-sulfonate (ANS) were purchased from Sigma Chemical Co. (St. Louis, MO, USA). All other reagents used were of analytical grade.

Protein Solution Preparation

pH measurements were carried out on Mettler Toledo pH meter (Seven Easy S20–K) using a Expert "Pro3 in 1" type electrode having the least count of the pH meter was 0.01 pH unit. The pH meter was routinely calibrated at room temperature with either 0.05 M potassium hydrogen phthalate buffer, pH 4.0 in the acidic range or 0.01 M tetraborate buffer, pH 9.2 in the alkaline range.

The buffers used for acid denaturation of conalbumin are at different pH values KCl/HCl (pH 0.8–1.4), Gly/HCl (pH 1.6–3.0), Sodium acetate (pH 3.5–5.0) and sodium phosphate (pH 6.0–7.0) buffer at a concentration of 20 mM. All the buffers were filtered through a 0.45-μm syringe filter.

Protein stock was prepared in 20 mM sodium phosphate buffer pH 7.0, and its concentration was measured by using the extinction coefficient at $E_{280\,nm}^{1\%} = 12.0$ [14] on Perkin

Elmer (Lambda 25) double beam spectrophotometer attached with Peltier temperature programmer (PTP–1). The molecular weight of conalbumin including glycochains was taken as 77 kDa.

CD Measurements

CD measurements were carried out with a Jasco spectropolarimeter (J–815) equipped with a Jasco Peltier-type temperature controller (PTC–424S/15). The instrument was calibrated with d-10-camphorsulphonic acid. Spectra were collected in a cell of 1 and 10 mm pathlength for far- and near-UV CD, respectively with scan speed of 100 nm/min and response time of 1 s. Each spectrum was the average of 2 scans. The CD results were expressed as MRE (mean residue ellipticity) in deg cm^2 dmol^{-1} which is defined as:

$$\text{MRE} = \theta_{obs}\big(10 \times n \times l \times c_p\big). \tag{1}$$

where θ_{obs} is the CD in milli-degree, n is the number of amino acid residues (705), l is the path length of the cell, and c_p is the mole fraction. The % α-helical content was calculated from the MRE values at 222 nm using the following equation as described by Chen et al. [15]:

$$\%\alpha - \text{helix} = (\text{MRE}_{222\,nm} - 2{,}340/30{,}300) \times 100. \tag{2}$$

The thermal unfolding of CA was carried out by measuring the temperature-dependent CD response at 222 nm from 25 to 95°C using a temperature rise of 1°C/min.

Data Analysis of Protein Denaturation

Temperature-induced unfolding curves were analyzed on the basis of two-state unfolding model. For a single-step unfolding process, $N \rightleftharpoons U$, where N is the native state and U is the unfolded state, the equilibrium constant K_u is

$$K_u = f_u/f_n. \tag{3}$$

With f_u and f_n being the molar fraction of U and N, respectively.

$$f_d = (Y_{obs} - Y_n)/(Y_u - Y_{obs}). \tag{4}$$

where Y_{obs}, Y_n and Y_u represent the observed property, the property of the native state and the property of unfolded state, respectively.

The change in free energy of unfolding in water ΔG_u°, is obtained by the linear extrapolation model [16]. The relationship between the denaturant and ΔG_u°, is approximated by the following equation:

$$\Delta G_u = -RT \ln K_u \tag{5}$$

and

$$\Delta G_u = \Delta G_u^\circ - m(T) \tag{6}$$

where m is the experimental measure of the dependence of ΔG_u on temperature, R is the gas constant (1.987 cal - deg^{-1} mol^{-1}), and T is the absolute temperature.

ΔG_u varies linearly as a function of pH with a proportionality factor m. Extrapolation of the extreme back to the pH value where the maximum folded population exists gives an estimate of the value of ΔG_u under that pH value, ΔG_u^{H+}[17]. The difference in free energy between the folded and unfolded states, ΔG_u, was calculated by the following equation:

$$\Delta G_u = \Delta G_u^{H+} - m(\text{pH}). \tag{7}$$

Tryptophanyl Fluorescence Measurements

Fluorescence measurements were performed on Hitachi spectrofluorometer (F-4500). The fluorescence spectra were measured at $25 \pm 0.1°$C with a 1-cm pathlength cell. The fluorescence was measured by exciting the protein at 295 nm, and emission spectra were recorded in the range of 300–400 nm. Both excitations an emission slits were set at 10 nm. Before performing, experiment solutions were incubated overnight at room temperature. The concentration of protein was kept at 2.5 μM with absorbance value of ~0.07, which was used throughout the fluorescence experiments to minimize the inner filter effect [18].

ANS-Binding Measurements

A fresh stock solution of ANS was prepared in distilled water, and its concentration was determined using molar extinction coefficient of $\epsilon M = 5{,}000$ M^{-1} cm^{-1} at 350 nm. For ANS-binding experiments, the molar ratio of protein to ANS was 1:50. The excitation wavelength was set at 380 nm, and the emission spectra were taken in the range of 400–600 nm. Both the excitation and emission slits were set at 10 nm.

Acrylamide-Quenching Experiments

In the quenching experiments, aliquots of 5 M quencher stock solution were added to protein solutions (2.5 μM) to achieve the desired range of quencher concentration (0.1–0.4 M). Excitation wavelength was set at 295 nm in order to excite tryptophan residues only, and the emission spectrum was recorded in the range 300–400 nm. The decrease in fluorescence intensity was analyzed by using the Stern–Volmer equation:

$$F_o/F = 1 + K_{sv}[Q] \tag{8}$$

$$K_{sv} = K_q \tau_o. \tag{9}$$

where F_o and F are the fluorescence intensities of the protein in the absence and presence of quenchers. K_{sv} is the quenching constant which was determined from the slope of the Stern–Volmer plot at lower concentrations of quencher, whereas [Q] represents molar concentration of quencher. K_q is the bimolecular rate constant of the quenching reaction, and τ_o is the average integral fluorescence life time of tryptophan which is $\sim4.31 \times 10^{-9}$ s.

Dynamic Light Scattering Measurements

DLS measurements were carried out at 830 nm by using DynaPro–TC–04 dynamic light scattering equipment (Protein Solutions, Wyatt Technology, Santa Barbara, CA) equipped with a temperature-controlled microsampler. Before measurements, all the solutions were spun at 10,000 rpm for 10 min and filtered through microfilter (Whatman International, Maidstone, UK) having an average pore size of 0.22 μm directly into a 12-μl black quartz cell, and protein concentration was 12.5 μM. Measured size was presented as the average value of 20 runs. All data analyses were analyzed by using Dynamics 6.10.0.10 software at optimized resolution. The mean hydrodynamic radius (R_h) and polydispersity (P_d) were estimated on the basis of an autocorrelation analysis of scattered light intensity data based on translational diffusion coefficient $\left(D_W^{25°C}\right)$ by Stokes–Einstein equation:

$$R_h = \frac{kT}{6\pi n D_W^{25°C}}. \tag{10}$$

where R_h is the hydrodynamic radius, k is the Boltzman's constant, T is the absolute temperature, η is the viscosity of water, and $D_W^{25°C}$ is the translational diffusion coefficient.

Results

Far-UV CD Studies

The acid-induced unfolded states contain significant amount of secondary structure as judged by far-UV CD measurements. The CD spectrum of native CA at pH 7.0 exhibited two minima at 208 and 222 nm, a character typical for α-helical structure (Fig. 1a). On moving toward acidic range, there occur marginal alternations in CD signals up to pH 3.0 as can be observed from nominal changes in the MRE value (see Table 1). This is also revealed by insignificant changes in % α-helix value. For native CA, the α-helical content is found to be 29%, whereas for acid-induced pre-MG and MG state, it comes out to be 26 and 23%, respectively. At pH 3.0, the CD spectrum of conalbumin is typical of unstructured protein because the minimum at ~200 nm has been observed in unstructured and class II β–proteins [19]. Moving further down to pH 1.0,
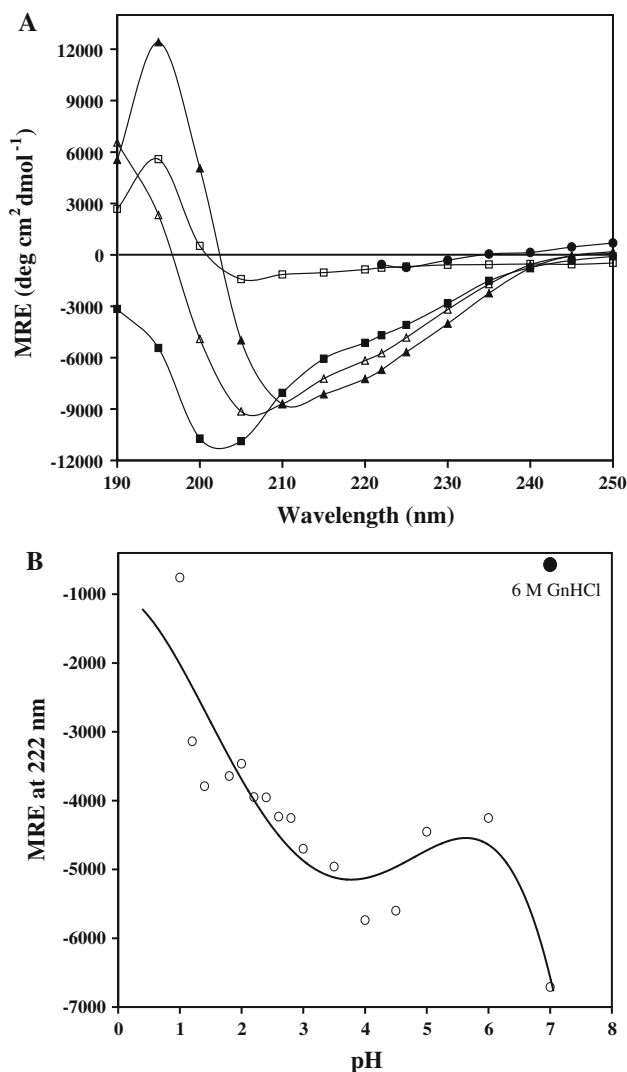
Fig. 1 **a** Far-UV CD spectra of CA native (*filled triangle*); pre-MG(*open triangle*); AI-MG (*filled square*) and acid-denatured (*open square*) states at pH 7.0, 4.0, 3.0 and 1.0, respectively. (*filled circle*) represents 6 M GnHCl denatured CA **b** MRE value of CA at 222 nm at different pH (*open circle*) and 6 M GnHCl (*filled circle*)

deviation from typical α-helical pattern takes place indicating loss of secondary structure. The maximum loss of secondary structure is observed at pH 1.0 (Fig. 1b). This is further confirmed from % α-helical content being reduced to 10. However, this deviated pattern is still similar from that obtained for protein incubated with 6 M GnHCl. These changes in secondary structure reflect that CA undergoes certain conformational changes in the acidic conditions.

Near-UV CD Studies

CD spectra in near UV region were used to examine the effect of decreasing pH on tertiary structure of CA. The intensities of aromatic CD bands depend upon the protein

rigidity with the more mobile side chains displaying lower intensities, the interaction between aromatic amino acids and the number of aromatic amino acid residues [20]. Additional evidence for structural instability can be gleaned from the near-UV CD spectra. The near-UV CD spectrum of the native state of CA reveals three negative ellipticity peaks at 277, 285 and 296 nm and single shoulder at 291 nm (MRE at 285 nm is -24 deg cm^2 d-mol^{-1}). In acidic condition (Fig. 2a), the intensity of the peak at these wavelengths responds quite differently to change in the pH. As can be observed, the peaks at 277, 285 and 291 nm tend to diminish with concomitant decrease in overall intensity as the pH decreases. There is decrease in the intensity as a result of decrease in MRE at the corresponding peaks and shoulders. MRE value at 285 nm initially increases with a decrease in the pH, reaching the maximum at pH 1.0 reaching -13 deg cm^2 dmol^{-1}. The structural changes observed at 285 nm could be attributed to the Trp environment, since Trp absorbs in this region. In Fig. 2b, the MRE at 285 nm also reveals an abrupt loss of sharp features at lower pH, indicating the loss of specific tertiary structures in extreme acidic conditions. The decrease in the peak intensity reflected subtle changes in the tertiary structure, which affected the environment of aromatic amino acid (Phe, Tyr and Trp) side chains [21]. These aromatic amino acid residues in the native structure disappeared in 6 M GnHCl indicating the disruption of the native tertiary structure. The shift of peak maxima and reduction of band intensity illustrates loss of native structure that indicates formation of a molten globule state.

Tryptophanyl Fluorescence

In proteins, Trp is highly sensitive to the polarity of its surrounding environment, and CA is a deca Trp-containing protein. Thus, microenvironmental modifications of CA aromatic residues due to denaturation by pH were studied by monitoring the changes in the fluorescence spectra as a function of pH. The emission maximum of CA under native condition was found to be 331 nm which undergone red shift of 9 nm at pH 3.0. This is suggestive of the solvent exposure of some of the Trp residues that were in the hydrophobic core of the protein under native condition. Fig. 3a shows spectra in the presence of 6 M GnHCl remains almost similar in shape to pH 3.0, but the emission maximum shifts to 350 nm which corresponds to the fluorescence maximum of tryptophan in aqueous solution (Fig. 3b). The pH-induced transition seems to be cooperative and exhibits a biphasic transition with first transition between pH 3.0 and 6.0 in the midst of pH 5.0 and the second between pH 1.0 and 2.0. Thermodynamic parameters for protein unfolding at lower pH were calculated from

Table 1 Spectroscopic and thermodynamic properties of CA

Properties	Native state (pH 7.0)	Pre-MG state (pH 4.0)	Acid-induced MG state (pH 3.0)	Acid-denatured state (pH 1.0)	Denatured state (6 M GnHCl at pH 7.0)
MRE 222 nm[a]	−6,710	−5,736	−4,700	−756	−569
MRE 285 nm[a]	−24	−12	−12	−13	−5
FI 331 nm[b]	361	265	218	34	227
λ_{max} nm	331	333	340	343	348
FI 480 nm[b]	72	1,944	2,415	22	29
λ_{max} nm	491	486	482	480	513
α-helix[c] (%)	29	26	23	10	9
Thermal unfolding 222 nm	Cooperative	Cooperative	Cooperative	Non-cooperative	Non-cooperative
T_m[d]	78°C	70°C	65°C	–	–
ΔG_u° (kcal mol^{-1})	59.6	53.1	46.6	38.6	13.3
m (kcal mol^{-1} M^{-1})	−0.76	−0.75	−0.72	−0.65	−0.39

[a] *MRE* value in deg cm^2 dmol^{-1} calculated by Eq. 1

[b] *FI* stands for fluorescence intensity in arbitrary units

[c] calculated by Chen et al. method Eq. 2

[d] T_m was calculated from thermal denaturation experiments

The free energy for unfolding ΔG_u°, obtained from two-state fits modal and is plotted as a function of temperature

the folded and unfolded fractions as mentioned in experimental section using Eqs. 3, 4, 5 and 7. The results in Fig. 3c show that the pH dependence of the free energy for unfolding of CA at 331 nm shows transition midpoint "pH$_m$" at pH 4.0. The values of free energy and "m" were calculated using Eq. 7 in the pH range of 4.5–3.0 and were on an average of −4.47 kcal mol^{-1} and 1.1 kcal mol^{-1} M^{-1}, respectively. Thus, decrease in pH makes protein structure more flexible and prone to acid-induced unfolding.

ANS-Binding Studies

The solvent exposure of the hydrophobic surface in CA at low pH was studied by ANS-binding experiments. Figure 4a shows fluorescence emission spectra of CA-ANS complex at different pH. The fluorescence intensity of CA-ANS was maximum at pH 3.0 in comparisons with that observed at pH 1.0, 4.0 and 7.0 (Fig. 4a). At pH 4.0, CA also shows the presence of solvent accessible hydrophobic patches due to increase in ANS binding, but it has less fluorescence intensity than at pH 3.0 which shows the presence of MG (at pH 3.0) and pre-MG (at pH 4.0). CA at low pH has enhanced solvent accessible clusters of hydrophobic regions, which were initially buried in the interior of native CA at pH 7.0. These results suggest the formation of a molten globule-like state in the unfolding pathway of CA is substantiated by the strong ANS binding in the acidic condition. Previously, molten globule states for several proteins under various denaturing conditions have been reported by our group [21, 22].

Thermal Unfolding

The effect of pH on the thermodynamic stability of CA was investigated by carrying out thermal unfolding which follows the changes in ellipticity at 222 nm which check the presence of residual secondary structure of CA. Figure 6 shows that F_d ploted against temperature was in a sigmoid fashion for pH 7.0, 4.0 and 3.0, but it showed a linear behavior at extreme acidic pH and 6 M GnHCl. This result indicates cooperativity at pH 7.0, 4.0, 3.0, and absence of cooperativity as expected for a non-compact structure at pH 1.0. The loss of signal in these cases is due to thermal unfolding of the hydrophobic cores or arises directly from reduction of the disulfide linkages in the protein. At pH 4.0, 3.0 and 1.0, the thermal unfolding curves showed smaller transition amplitudes than the native which has T_m of 78°C. The curve shows a single-phase transition having estimated T_m of 78°C (at pH 7.0), which is close to T_m of 81°C obtained using microcalorimetry (DSC) [23]. The free energy for unfolding is fairly sensitive to the changes in environment and was calculated using Eq. 6 (Table 1). The native CA exhibits highest free energy $\left(\Delta G_u^\circ\right)$ 59.6 kcal mol^{-1}, whereas 6 M GnHCl exhibits the lowest ΔG_u° (13.3 kcal mol^{-1}). The "m-values" appear to decrease slightly with decrease in pH, suggesting that the variation in "m-values" is believed to be due to change in the solvent accessible area of hydrophobic residues. In spite of these large differences in stability, pH dependence of the denaturation temperature of CA was observed revealing a broad maximum at pH ranging from 3.0 to 7.0, but the maximum stability coinciding with neutral, and at
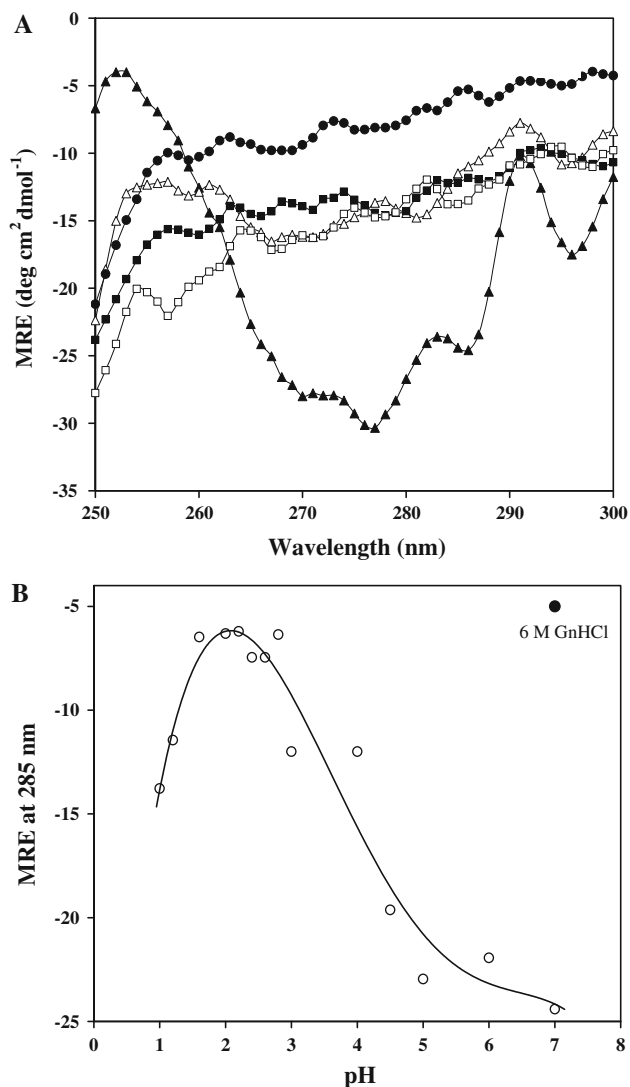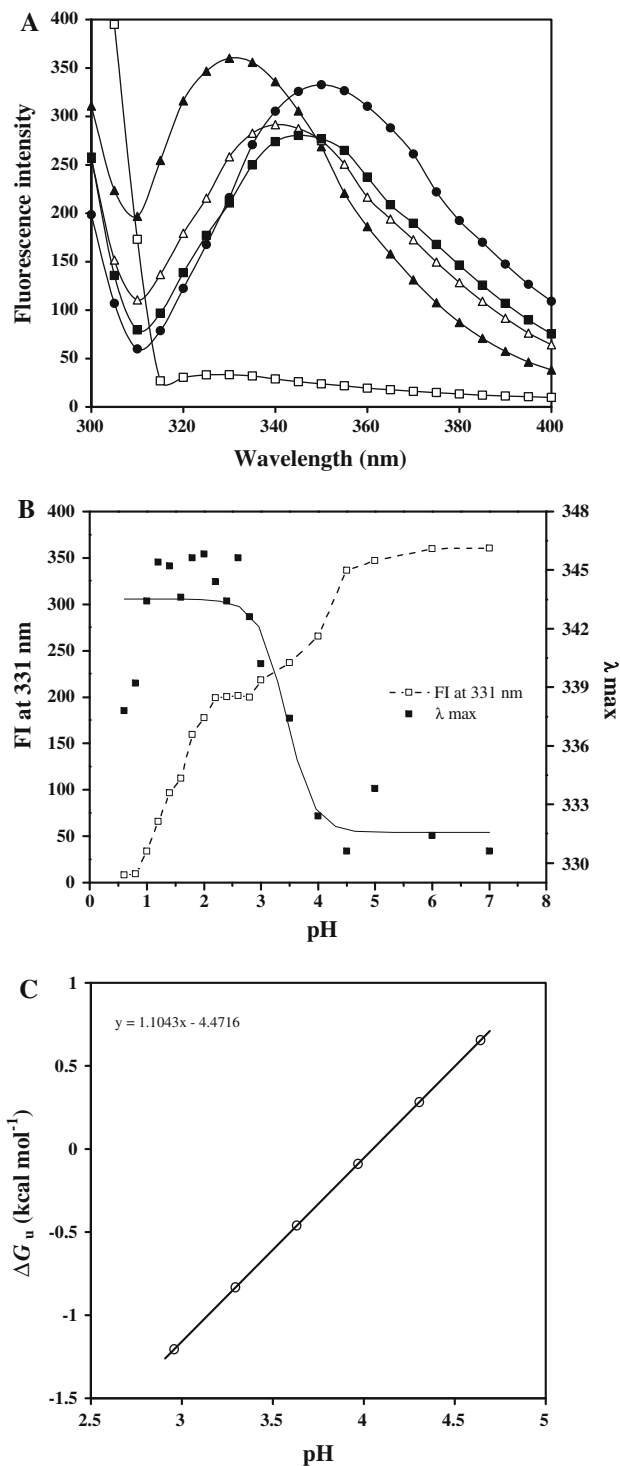
Fig. 2 **a** Near-UV CD spectra of CA at pH 7.0 (*filled triangle*), 4.0 (*open triangle*), 3.0 (*filled square*), 1.0 (*open square*) and 6 M GnHCl denatured (*filled circle*). **b** MRE value of CA at 285 nm at different pH (*open circle*) and 6 M GnHCl (*filled circle*)
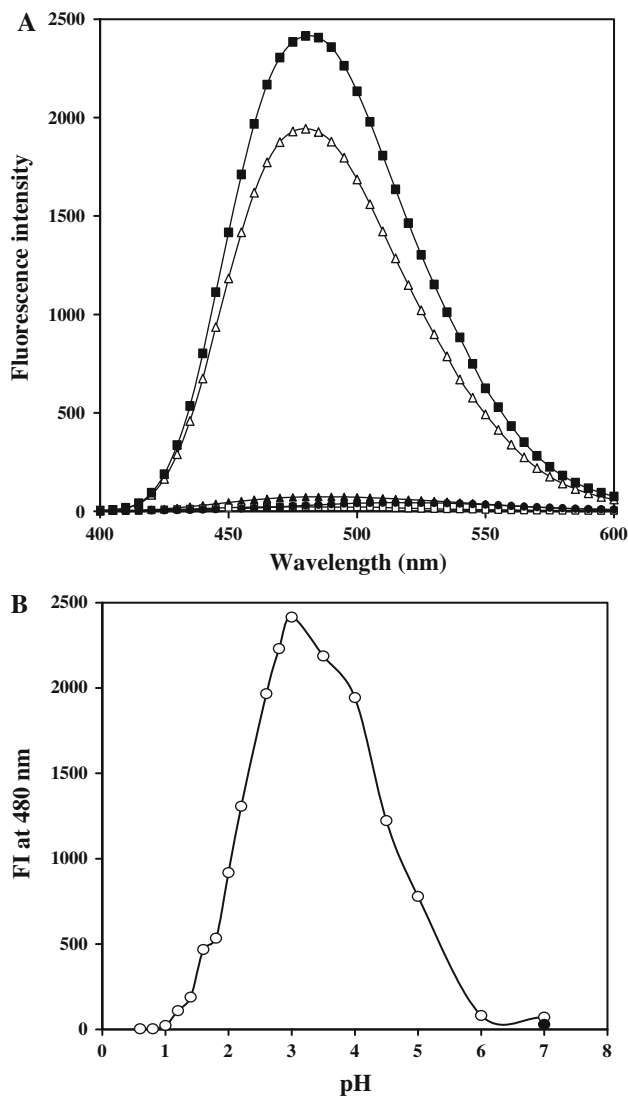
pH near its isoelectric point of 6.85. The maximum conformational stability of CA at zero net charge could be due to the favorable electrostatic interactions among the positive and negative charged groups arranged on the surface of protein as a consequence of decreasing the surrounding effective dielectric constant causes the decrease in stability.

Acrylamide Quenching

Quenching of tryptophan fluorescence by acrylamide was carried out for pH 7.0, 4.0, 3.0, 1.0 and 6 M GnHCl-induced states. Acrylamide is an appropriate choice as a quenching agent because it is a neutral molecule. The
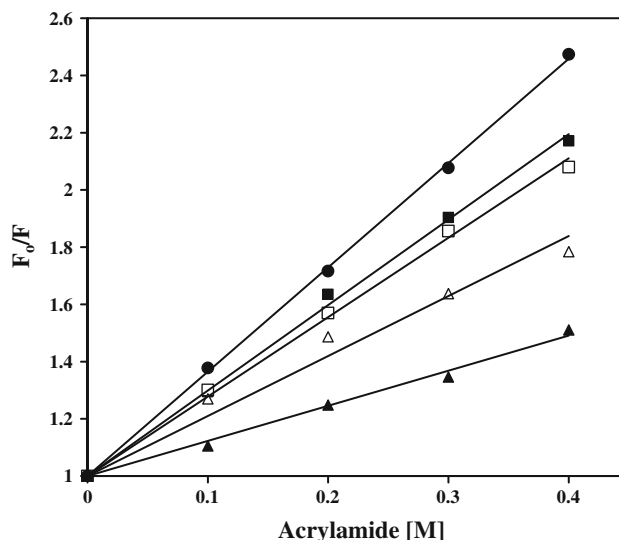

Fig. 3 **a** Tryptophan fluorescence emission spectra of CA at pH 7.0 (*filled triangle*), 4.0 (*open triangle*), 3.0 (*filled square*), 1.0 (*open square*) and 6 M GnHCl denatured (*filled circle*) **b** Fluorescence intensity at 331 nm (*open square*) and λmax (*filled square*) of CA as a function of pH. The protein was excited at 295 nm. **c** Variation of free energy parameters of unfolding with pH dependence of FI at 331 nm
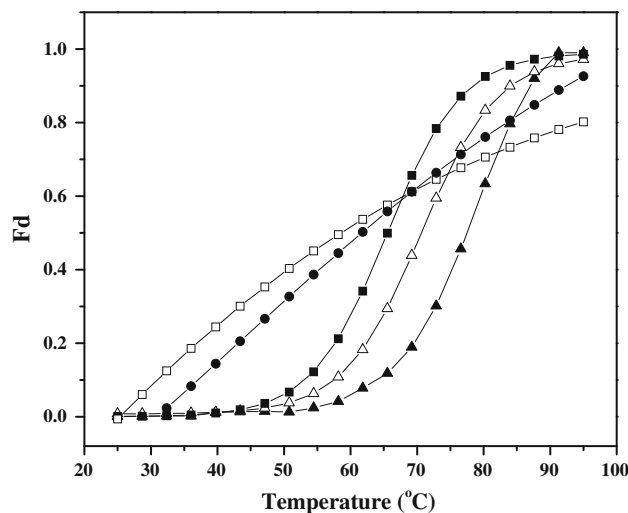
Fig. 5 Stern-Volmer plots for acrylamide quenching of tryptophan fluorescence of CA. (for captions refer to Fig. 6)

Fig. 4 a Fluorescence emission spectra of CA-ANS complex at pH 7.0 (*filled triangle*), 4.0 (*open triangle*), 3.0 (*filled square*), 1.0 (*open square*) and 6 M GnHCl denatured (*filled circle*); **b** Fluorescence intensity of CA-ANS complex at 480 nm; at different pH (*open circle*) and 6 M GnHCl (*filled circle*). The protein was excited at 380 nm

Fig. 6 Temperature-induced denaturation profile showing changes in ellipticity at 222 nm of CA at pH 7.0 (*filled triangle*), 4.0 (*open triangle*), 3.0 (*filled square*), 1.0 (*open square*) and 6 M GnHCl denatured (*filled circle*)

extent of quenching by acrylamide was estimated by K_{sv} and K_q that were calculated by plotting linear Stern–Volmer plot between F_o/F and acrylamide concentration (Fig. 5). The K_{sv} is reported as the slope of the line which reflects the accessibility of tryptophan residues to collisions with acrylamide [24]. The quenching parameters obtained by analyses of Stern–Volmer plots are presented in Table 2. The K_{sv} value of native CA was found to be 1.22 M^{-1}; the corresponding values of K_{sv} for pre-MG (at pH 4.0) and MG (at pH 3.0) state were higher than native CA (2.09 and 2.77 M^{-1}). This suggests that the Trp residues of CA become less accessible to the quenchers in native condition while increased exposure in the molten globule state which clearly indicates that the molten globule state is partially

unfolded, exposing tryptophan residues to collisions with acrylamide in accordance with the red shift observed for the wavelengths at the emission maximum. In addition, the K_q values in each case of states are in the range of 10^8 M^{-1} s^{-1} (Table 2) which is 100 time lower than the maximum value for dynamic quenching, 2×10^{10} M^{-1} s^{-1} indication of the dynamic quenching [24].

Hydrodynamic Parameters Determination of CA

The translational diffusion coefficient $\left(D_W^{25°C}\right)$ is one of the useful physical properties for characterizing the nature of

**Table 2** Acrylamide quenching data of CA in different states

State	pH	$K_{sv}[M^{-1}]$	$K_q[M^{-1}s^{-1}]$
Native state	7.0	1.22	2.8×10^8
AI-pre-MG state	4.0	2.09	4.8×10^8
AI-MG state	3.0	2.77	6.2×10^8
AI-denatured state	1.0	2.98	6.9×10^8
6 M GnHCl denatured state	7.0	3.64	7.5×10^8

K_{sv} and K_q calculated by Eqs. 8 and 9, respectively

Table 3 pH dependence comparison of the hydrodynamic radii (R_h) and translational diffusion coefficients $\left(D_W^{25°C}\right)$ from dynamic light scattering (DLS) experiments describing different states of CA

State	pH	App. M.W. [kDa]	R_h [nm]	$D_W^{25°C}$ [cm^2 s^{-1}]	P_d [%]
Native state	7.0	212	5.1	4.69×10^{-7}	28.4
AI-Pre-MG state	4.0	140	4.8	4.89×10^{-7}	17.7
AI-MG state	3.0	99	4.7	4.91×10^{-7}	18.3
AI-denatured state	1.0	226	6.0	3.99×10^{-7}	23.4
6 M GnHCl denatured	7.0	1,564	13.8	1.75×10^{-7}	26.0

molecules in solution phase. This value reflects not only the molecular size or solution viscosity but also intermolecular interactions between a diffusing molecule and water molecules (hydrogen bond networks). Since hydrogen bond networks are sensitive to conformation, thus $D_W^{25°C}$ also reflects conformation of a protein. Values of the translational diffusion coefficient $\left(D_W^{25°C}\right)$ were obtained directly using value of hydrodynamic radii from Eq. 10. At pH 7.0, hydrodynamic radius (R_h) was found to be equal to 5.1 nm which gave value of $D_W^{25°C}$ of native CA equal to 4.69×10^{-7} cm^2 s^{-1}. At pH 4.0, CA has slightly smaller hydrodynamic radius of 4.8 nm which corresponds to value of $D_W^{25°C}$ equivalent to 4.89×10^{-7} cm^2 s^{-1}. The R_h values are 4.7 and 6.0 nm for pH 3.0 and pH 1.0, respectively. $D_W^{25°C}$ for pH 3.0 and pH 1.0 were 4.91×10^{-7} and 3.99×10^{-7} cm^2 s^{-1}, respectively (Table 3) and were slightly higher than the calculated values from Stokes–Einstein equation 3.09×10^{-7} and 3.61×10^{-7} cm^2 s^{-1} correspondingly. It can be clearly seen from Fig. 7 that on decreasing the pH, the $D_W^{25°C}$ increases while the R_h decreases suggesting that acidic pH induced changes in the CA molecules that indirectly change local diffusion coefficient through hydrodynamic effects. The changes in above results are indicative of the acid-induced dissociation of CA molecule [22].
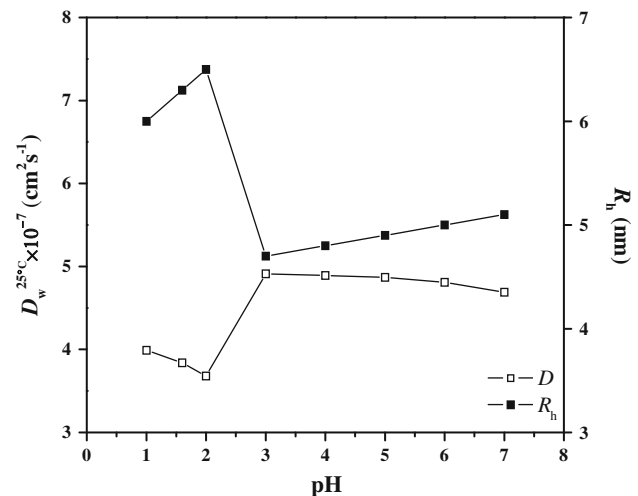
Fig. 7 Trends of the translational diffusion coefficients $\left(D_W^{25°C}\right)$ and the hydrodynamic radii (R_h) for CA as a function of pH

Discussion

The net charge on CA molecule at neutral pH is $(-)$ 1, because of the negative charge on side chains of Asp and Glu, positive charge on side chains of Lys and Arg and partial positive charge on side chain of His residue [25]. Protein structures are stabilized with various non-covalent interactions such as hydrophobic, electrostatic, van der Waals and hydrogen bonds but found to be significantly affected by acidic pH. This is due to the presence of both attractive and repulsive charge–charge-motivated interactions that are present in the proteins. When a protein unfolds, the charges on amino acid residues are away from each other and thus effective dielectric constant increased and consequently coulombic interactions substantially reduced. So, in general, coulombic interactions contribute favorably to upholding structural stability of the proteins [26]. During acid-induced denaturation of proteins, ionisable side chains of the protein get protonated due to elevation in H$^+$ which facilitates the formation of a premolten globule and molten globule state. Further increase in H$^+$ cause resultant charge–charge repulsion which consequently leads to protein unfolding and formation of acid-denatured state and thereafter decrease in pH has no effect on ionization state of protein but increases anion concentration [27, 28].

Acid-induced unfolding of CA was followed by far-UV CD, near-UV CD, intrinsic and extrinsic fluorescence measurement and hydrodynamic parameters determination.

The secondary structural changes on pH variation were measured using far-UV CD that is non-cooperative with two well-distinct transitions. The first transition between pH 7.0 and 4.0 involves conversion of native protein into

acid-unfolded state with residual secondary structure, followed by second transition corresponding to formation of secondary structure. Acid-induced molten globule state is populated at pH 3.0 in this second transition with CD spectra comparable to that of native state. Molar ellipticity value at 222 nm in MG state is $-4,700$ deg cm^2 dmol^{-1} which is lower than that of the native protein at pH 7.0 (-6710 deg cm^2 dmol^{-1}). Retention of considerable amount of secondary structure is a prerequisites for MG state [20, 22].

The tertiary structural alteration with pH was analyzed by intrinsic and extrinsic fluorescence spectroscopy and near-UV CD. The Trp residue appears to sit in a different environment at different pH condition. CA undergoes a native to molten globule transition at pH 3.0 while the unfolded state of CA populated at pH 1.0 as evident by decrease in emitted fluorescence intensity together with red shift in maximum emission wavelength. As the pH decrease, CA unfolds to form acid-induced pre-MG state and to MG state directly at lower pH. This is similar to MG state of maltose binding protein (MBP), a large monomeric two domain protein, where MG state was populated at acidic pH 3.0 [29]. Furthermore, Figs. 1a and 3a confirm that considerable amounts of unstructured species were present at pH 1.0. Near-UV CD data also confirm the loss of tertiary structure at pH 3.0. Tertiary structural perturbations induced by pH which are also manifested by ANS binding. ANS binds maximally to CA at acid-induced MG state at pH 3.0 relative to native and denatured state. At lower pH values, decrease in magnitude of ANS binding occurs. An increase in extrinsic fluorescence intensity together with blue shift as compared to native suggests increase in hydrophobicity of the protein at pH 3.0. Disrupted tertiary structure of the protein at pH 3.0 together with exposed hydrophobic patches confirms that observed properties agree with the definition of molten globule state.

To further understand the difference in pH dependence structural changes, we performed an acrylamide quenching experiment comparing the effect of varying acrylamide concentration on CA at different pH conditions. Our acrylamide quenching data at lower pH values show a lower

K_{sv} values compared with 6 M GuHCl denatured protein whereas higher value of K_{sv} than the native state of protein. These results reflected that hydrophobic pockets harboring the major emitting tryptophan(s) are present in both pre-molten globule and molten globule conformations.

The mean residue ellipticity at 222 nm as a function of temperature as illustrated in Fig. 6 shows the equilibrium unfolding of the protein at different pH values. The results clearly suggest that decrease in pH decreases the stability of the protein toward thermal unfolding significantly. In our study, T_m is found to be pH dependent and decreases with increase in positive net charge of the protein; thus, it appears that some of the interactions stabilizing the compactly folded conformation are disrupted in MG-like state. These results suggest that the protein in the MG-like state is significantly less stable than the folded state which is characteristic feature of MG state.

In DLS analyses, it was studied that the mean hydrodynamic size changes due to change of the pH values of the medium. We observed decrease in $D_W^{25°C}$ and an increase in hydrodynamic radii (R_h) on decreasing pH. The size expansion could occur due to the increase in net positive charge. At pH 1.0, the CA molecules are in expanded phase, and its more easily accessible charged groups are highly solvated (i.e., hydrated) which cause increase in the R_h of the protein in the solution. Additionally, there occurs decrease in the diffusion constant on increasing protonation (H$^+$). The $D_W^{25°C}$ reflects not only the molecular size or solution viscosity but also intermolecular interactions between a diffusing molecule and water molecules (hydrogen bond networks). Since hydrogen bond networks are sensitive to conformation, thus $D_W^{25°C}$ also reflects conformation of a protein.

So it can be concluded from all results taken together that at pH 3.0 CA exists as MG while at pH 4.0, it exists as pre-MG. Furthermore, it is already reported that C-domain linking residues 478–671 are susceptible for denaturation and are assumed to be more exposed, so we proposed that residues of C-domain underwent unfolding first on decreasing pH [10]. This description is further explained by schematic representation of acid-induced unfolding of CA (Fig. 8).

Fig. 8 A schematic representation of the proposed unfolding pathway of CA, native, pre-MG, MG, acid-induced denatured and 6 M GnHCl denatured states
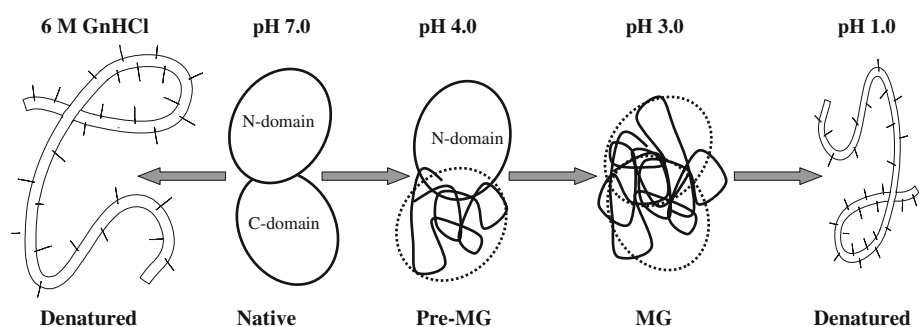
Conclusion

Understanding of protein stability is important under preservation processes. Heat and acids are two major reasons for protein deactivation as they affect primary, secondary, tertiary and quaternary structures. In this study, we identified and characterized the stable MG-like state accumulated in acidic region at pH 3.0. Furthermore, our study gives an insight into unfolding mechanism of CA under harsh environment like acidic environment which has large application in the feed industry, pharmaceuticals, veterinary medicines, clinics for human, etc.

References

1. Ptitsyn, O. B., Pain, R. H., Semisotnov, G. V., Zerovnik, E., & Razgulyaev, O. I. (1990). Evidence for a molten globule state as a general intermediate in protein folding. *FEBS Letters, 262,* 20–24.
2. Arai, M., Ito, K., Inobe, T., Nakao, M., Maki, K., Kamagata, K., et al. (2002). Fast compaction of alpha-lactalbumin during folding studied by stopped-flow X-ray scattering. *Journal of Molecular Biology, 321,* 121–132.
3. Hsieh, H. C., Kumar, T. K., Chiu, C. C., & Yu, C. (2005). Equilibrium unfolding of an oligomeric protein involves formation of a multimeric intermediate state(s). *Biochemical and Biophysical Research Communications, 326,* 108–114.
4. Sridevi, K., Lakshmikanth, G. S., Krishnamoorthy, G., & Udgaonkar, J. B. (2004). Increasing stability reduces conformational heterogeneity in a protein folding intermediate ensemble. *Journal of Molecular Biology, 337,* 699–711.
5. Nishimura, C., Dyson, H. J., & Wright, P. E. (2008). The kinetic and equilibrium molten globule intermediates of apoleghemoglobin differ in structure. *Journal of Molecular Biology, 378,* 715–725.
6. Paci, E., Greene, L. H., Jones, R. M., & Smith, L. J. (2005). Characterization of the molten globule state of retinol-binding protein using a molecular dynamics simulation approach. *FEBS Journal, 272,* 4826–4838.
7. Chen, B. L., Baase, W. A., Nicholson, H., & Schellman, J. A. (1992). Folding kinetics of T4 lysozyme and nine mutants at 12°C. *Biochemistry, 31,* 1464–1476.
8. Nakao, M., Maki, K., Arai, M., Koshiba, T., Nitta, K., & Kuwajima, K. (2005). Characterization of kinetic folding intermediates of recombinant canine milk lysozyme by stopped-flow circular dichroism. *Biochemistry, 44,* 6685–6692.
9. de Sousa Rde, C., Coimbra, J. S., da Silva, L. H., da Silva, Mdo. C., Rojas, E. E., & Vicente, A. A. (2009). Thermodynamic studies of partitioning behavior of lysozyme and conalbumin in aqueous two-phase systems. *Journal of Chromatography B, 877,* 2579–2584.
10. Stevens, L. (1996). Egg proteins: What are their functions? *Science Progress, 79,* 65–87.
11. Ko, K. Y., Mendonca, A. F., & Ahn, D. U. (2008). Influence of zinc, sodium bicarbonate, and citric acid on the antibacterial activity of ovotransferrin against *Escherichia coli* O157:H7 and *Listeria monocytogenes* in model systems and Ham. *Poultry Science, 87,* 2660–2670.
12. Stevens, L. (1991). Egg white proteins. *Comparative Biochemistry and Physiology B, 100,* 1–9.
13. Kelly, S. M., & Price, N. C. (2000). The use of circular dichroism in the investigation of protein structure and function. *Current Protein & Peptide Science, 1,* 349–384.
14. Woodworth, R. C., & Schade, A. L. (1959). Conalbumin: a rapid, high-yield preparation from egg white. *Archives of Biochemistry and Biophysics, 82,* 78–82.
15. Chen, Y. H., Yang, J. T., & Martinez, H. M. (1972). Determination of the secondary structures of proteins by circular dichroism and optical rotatory dispersion. *Biochemistry, 11,* 4120–4131.
16. Pace, C. N., & Scholtz, M. (1997). Protein Structure, A Practical Approach. In T. E. Creighton (Ed.), *Measuring the conformational stability of a protein* (p. 383). New York: Oxford University Press.
17. Ahmad, E., Rahman, S. K., Khan, J. M., Varshney, A., & Khan, R. H. (2010). *Phytolacca americana* lectin (Pa-2; pokeweed mitogen): An intrinsically unordered protein and its conversion into partial order at low pH. *Bioscience Reports, 30,* 125–134.
18. Larsson, T., Wedborg, M., & Turner, D. (2007). Correction of inner-filter effect in fluorescence excitation-emission matrix spectrometry using Raman scatter. *Analytica Chimica Acta, 2,* 357–363.
19. Venyaminov, S. Y., & Yang, J. T. (1996). In G. D. Fasman (Ed.), *Circular dichroism and the conformational analysis of biomolecules* (pp. 69–109). New York: Plenum Press.
20. Kelly, S. M., & Price, N. C. (1997). The application of circular dichroism to studies of protein folding and unfolding. *Biochimica et Biophysica Acta, 1338,* 161–185.
21. Varshney, A., Ahmad, B., Rabbani, G., Kumar, V., Yadav, S., & Khan, R. H. (2010). Acid-induced unfolding of didecameric keyhole limpet hemocyanin: detection and characterizations of decameric and tetrameric intermediate states. *Amino Acids, 39,* 899–910.
22. Ahmad, E., Fatima, S., Khan, M. M., & Khan, R. H. (2010). More stable structure of wheat germ lipase at low pH than its native state. *Biochimie, 92,* 885–893.
23. Rossi, M., & Schiraldi, A. (1992). Thermal denaturation and aggregation of egg proteins. *Thermochimica Acta, 199,* 115–123.
24. Eftink, M. R., & Ghiron, C. A. (1987). Does the fluorescence quencher acrylamide bind to proteins? *Biochimica et Biophysica Acta, 3,* 343–349.
25. Hanakam, F., Gerisch, G., Lotz, S., Alt, T., & Seelig, A. (1996). Binding of hisactophilin I and II to lipid membranes is controlled by a pH-dependent myristoyl-histidine switch. *Biochemistry, 35,* 11036–11044.
26. Grimsley, G. R., Shaw, K. L., Fee, L. R., Alston, R. W., Huyghues-Despointes, B. M., Thurlkill, R. L., et al. (1999). Increasing protein stability by altering long-range coulombic interactions. *Protein Science, 8,* 1843–1849.
27. Fink, A. L., Calciano, L. J., Goto, Y., Kurotsu, T., & Palleros, D. R. (1994). Classification of acid denaturation of proteins: Intermediates and unfolded states. *Biochemistry, 33,* 12504–12511.
28. Pace, C. N., Alston, R. W., & Shaw, K. L. (2000). Charge-charge interactions influence the denatured state ensemble and contribute to protein stability. *Protein Science, 9,* 1395–1398.
29. Sheshadri, S., Lingaraju, G. M., & Varadarajan, R. (1999). Denaturant mediated unfolding of both native and molten globule states of maltose binding protein are accompanied by large delta Cp's. *Protein Science, 8,* 1689–1695.